Available online at www.sciencedirect.com

ScienceDirect

journal homepage: www.elsevier.com/locate/he

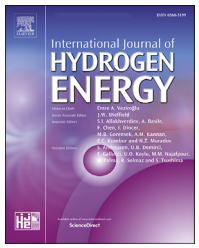

Hydrogen storage in $Zr_{0.9}Ti_{0.1}(Ni_{0.5}Cr_{0.5-x}V_x)_2$ Laves phase, with x = 0, 0.125, 0.25, 0.375, 0.5. A theoretical approach

A. Robina [a,b], P. Bechthold [b], A. Juan [b], C. Pistonesi [b], M.E. Pronsato [b,*]

[a] Facultad de Ingeniería, Universidad Nacional de La Patagonia San Juan Bosco, Ciudad Universitaria, (9005), Comodoro Rivadavia, Chubut, Argentina

[b] Instituto de Física Del Sur (IFISUR, UNS–CONICET) and Departamento de Física, Universidad Nacional Del Sur, Av. Alem 1253, B8000CPB, Bahía Blanca, Argentina

ARTICLE INFO

Article history:
Received 26 April 2018
Received in revised form
14 June 2018
Accepted 23 June 2018
Available online 14 July 2018

Keywords:
Laves phases
Hydrogen
Storage
DFT

ABSTRACT

Density functional calculations were performed on $Zr_{0.9}Ti_{0.1}(Ni_{0.5}Cr_{0.5-x}V_x)_2$ Laves Phase, with x = 0, 0.125, 0.25, 0.375 and 0.5, in order to study its H absorption capacity. Binding energy, electronic structure and bonding were analyzed for the intermetallic compound with different V content and increasing amounts of hydrogen.

The optimized geometry was found in good agreement with experimental data of the C14 Laves phase. Hydrogen locates preferentially in A_2B_2 tetrahedral sites in the AB_2 matrix (A = Zr, Ti; B = Ni, Cr, V) but AB_3 and B_4sites are also stable. The volume of the intermetallic and the H binding energy increases with vanadium content. Theoretically H absorption is possible up to 4.5 H/F.U. but the strongest binding energy is achieved with 3 H/F. U.

The main contribution to density of states is due to d states of all components of the structure and an H-metal bonding is observed in the range −10 to −4 eV.

Introduction

There will come a day when fossil fuels all eventually run out since they are non renewable energy resources. With this unavoidable scene and the need to create a greater environmental awareness comes the search for more efficient and cleaner energies technologies and ways to store and transport them. Several alternatives are based on hydrogen, seen as the promising and ideal mean of energy storage in a comprehensive clean-energy concept. Although hydrogen has the highest energy density, it also has the lowest volumetric storage density, which is the most remarkable disadvantage and challenging task nowadays to establish and promote a global hydrogen economy system. Despite this fact, different techniques of storing hydrogen have been developed among which some special intermetallic compounds play a crucial role. In essence, AB_2-type alloys, also known as Laves phases, have been extensively studied since 1980's as the active materials for the negative electrode in Nickel Metal Hydride (NiMH) batteries due to their suggestive behavior as solid state hydrogen materials [1]. In this kind of applications, the negative electrode is generally made of alloys of two or more metallic elements with narrow bands of integer stoichiometries. Depending on their composition and crystal structure, these materials have components which can each consist of a

* Corresponding author.
E-mail address: pronsato@criba.edu.ar (M.E. Pronsato).
https://doi.org/10.1016/j.ijhydene.2018.06.131

number of different elements in varying ranges of stoichiometry (mostly recognized as *mischmetals* or multielement, multiphase and compositionally disordered alloys) that facilitate hydrides formation. Thus the variation of the components of metal hydrides allows the *design of materials* with the desired characteristics for battery performance, such as low equilibrium pressure, resistance to corrosion, mechanical stability, reversibility and hydrogen storage ability. Here the cost of the substituted elements is also a major parameter for developing new materials. Ovshinsky and coworkers introduced the multielement, multiphase, and compositionally disordered *alloy design concept* to lead the way to the successful commercialization of the NiMH battery technology which performance closely depends on the characteristics of the hydride-forming alloy. To ensure the reversibility of the systems, an important aspect of the MH design is the range of metal-to-hydrogen (M − H) bond strengths, which should be between 25 and 50 kJ/mol (0.259–0.518 eV) [2–4].

Hydrogen absorption capacity of AB_2 alloys based on Zr as negative electrodes for Ni-MH batteries are, precisely, the main subject of this work. Many authors have recently investigated, both theoretically and experimentally, the hydrogen behavior within various crystal structures and how their atomic arrangements change when different chemical replacements take place, as well as the absorption ratios [5–8].

Laves phases can crystallize in one of three different structures types with the following representative forms: hexagonal C14 $MgZn_2$ and C36 $MgNi_2$ and cubic C15 $MgCu_2$ [9–12]. The only determining geometric factor is the atomic radius ratio between A and B elements. When $\frac{r_A}{r_B} \cong \frac{\sqrt{3}}{\sqrt{2}} \cong 1.2$ both A and B atomic nets merge in a very efficient and compact way where each A atom is surrounded by 12 neighbors and each B atom by 6 [13]. In particular, the C14 structure has a $P6_3/mmc$ (D^4_{6h}) symmetry with four formula unit per unit cell (4 F.U./U.C) and a c/a ratio of $(8/3)^{1/2}$. These compounds are also tetrahedrally close-packed (TCP) [14]. The C14 structure presents three distinct types of tetrahedral interstices per AB_2 formula available for storing hydrogen: 12 A_2B_2 sites, 4 AB_3 sites and 1 B_4 site [15].

In a previous work [16], we have found that $Zr(Cr_{0.5}Ni_{0.5})_2$ C14 Laves phase was energetically more stable for hydrogen storage than $ZrCr_2$, owing to the partial replacement of Cr by Ni atoms.

Effects of partial replacement of certain A and B atoms in AB_2 Laves phases structures and their hydrogen-sorbing rates have been studied previously. Yang X. G. et al. [17] studied the effect of alloying with Ti, V and Mn on the electrochemical properties of Zr–Cr–Ni based Laves phases metal hydride electrodes, showing that the partial substitution of Ni and Cr in the alloy by V and Mn elements in the range 0.7–1.0 per AB_2 formula improves the hydrogen storage and electrochemical capacities of the alloy. Verbetsky et al. [18] analyzed the absorption and electrocatalytical properties of electrodes based on C14 $Zr_{0.5}Ti_{0.5}V_{0.5}Ni_{1.3}Cr_{0.2}$ with Cu binder. They found that this alloy composition displayed a high discharge capacity and could be a good candidate material for fabricating MH-electrodes for batteries. Also in order to determine its possible application as negative electrodes in NiMH rechargeable batteries, Visintin et al. [19] explored the hydrogen absorption characteristics and electrochemical properties of $Zr_{1-x}Ti_xCrNi$ Laves phase by volumetric and electrochemical techniques. They could ensure that $Zr_{0.9}Ti_{0.1}CrNi$ alloy electrode exhibited the highest discharged capacity and the best performance during fast charge-discharge cycling. At the same time, Peretti et al. [20] demonstrated hydrogen absorption behavior results in $Zr_{0.9}Ti_{0.1}NiMn_{0.5}Cr_xV_{0.5-x}$ alloys by experimental techniques. They concluded that the hydrogen absorption capacity of the phase decreases on increasing the Cr/V content ratio and the alloy obtained with $x = 0.25$ optimized the compromise between a high discharge capacity without significant increase of the high rate discharge ability, showing a high hydrogen storage capacity (H/F.U. ≈ 3.6) too.

In this work, following the same goal and with the aim to find a better multi-component design, we analyze five different C14 Laves phases alloys with fixed Zr, Ti and Ni and variable Cr and V composition.

Crystal models and computational method

It is well known that $ZrCr_2$ alloy presents a high hydrogen storage capacity (3.4 H/F.U.); nevertheless, its technological applications are prevented by the strong stability of the hydrides at room temperature. Previous investigations have concluded that partial substitution of Cr by other transitions metals of the first period -like Ni-may affect the dissociation equilibrium pressure and contribute to destabilize the hydride [21,22]. In the present research and in accordance with our latest study [16], half of Cr atoms of the alloy are replaced by Ni atoms while the other half is gradually replaced by V atoms. Vanadium is a room temperature hydrogen storage element with the capability to significantly increase the average metal-hydrogen bond strength and lower the phase equilibrium pressure (qualities that are absent for other B-site atoms such as Co, Mn, Al, Sn, Fe). In addition, its relatively large atomic radius makes it the first B-atom reported to occupy an A-site in an over-stoichiometric situation [23]. This V atom in an A-site substitution increases the degree of disorder and also makes more hydrogen interstitial sites available for reversible hydrogen storage [24]. With respect to the A component, it is also expected that partial substitution of Zr by Ti results in a further increase in the dissociation pressure due to the smaller atomic radius of Ti that leads to a decrease in the lattice parameter and hence to more instability of the hydrides. However, it is worth noting that PCT curves of Ti substituted Zr-based AB_2 alloys show that the increase in Ti content also decreases the hydrogen storage capacity. This is why the substitution of only a limited amount of Zr by Ti contributes to reduce the hydride stability while preserving a relatively good hydrogen storage capacity in weight percentage and increasing the plateau pressure of the alloy [19,21,25]. Consistent with this, we choose to study a $Zr_{0.9}Ti_{0.1}$ composition as it is the combination that revealed a good performance on AB_2 type alloys [19,26].

We will study five Laves phases alloys $Zr_{0.9}Ti_{0.1}(Ni_{0.5}Cr_{0.5-x}V_x)_2$, with $x = 0$, 0.125, 0.25, 0.375 and 0.5 by the Density Functional Theory (DFT) calculations with the intention of reporting changes in hydrogen binding energies, electronic charge distribution and magnetic moments as different H concentrations are considered for each case.

To simulate and represent all substitutions in the correct proportion, we built a supercell consisting of 4 originals unit cells (Fig. 1). This new cell is composed by 32 F.U./U.C. and has a total of 544 interstitial sites for hydrogen storage of which 384 are A_2B_2 type, 128 AB_3 and 32 B_4 (each type of site is indicated in the 2 × 2 × 2 supercell shown in Fig. 1). Despite this large number of possibilities, electrostatic limitations prevent a complete hydriding and most sites remain unoccupied.

It is important to highlight that until today no material has been found with properties fulfilling both criterion: the energetic one, related to the gravimetric hydrogen density and the thermodynamic one, associated with hydride materials with improved thermodynamical properties. Therefore, the search continues and new combinations of metals in these intermetallics are proposed, prepared and tested experimentally and predicted theoretically.

All calculations were performed using the Density Functional Theory (DFT) implemented in the Vienna Ab-initio Simulation Package (VASP) [27]. This code employs a plane wave basis set and a periodic supercell method [28–30]. The Kohn-Sham equations were solved variationally using the projected-augmented method (PAW) [31] and the exchange and correlation energies were calculated using the Perdew, Burke and Ernzerhof (PBE) form of the spin-polarized generalized gradient approximation (GGA) [32]. The convergence in total energy and the force on the atoms were set less than 10^{-4}eV and 10^{-3} eV/Å, respectively. To sample the Brillouin Zone in hexagonal lattices a 3 × 3 × 3 Gamma (Γ-point) centered grid method was used. All simulations were performed using an energy cut-off of 450 eV for the plane wave basis set. Geometry optimizations for all systems were carried out in two steps: first, the volume of the supercell was relaxed keeping the relative position of ions fixed. Then, ions were allowed to relax within the cell.

From total energy values extracted from the geometry optimization results, the H binding energy in the hydrides systems can be express as:

$$E_B = 1/n[E(AB_2 + nH) - E(AB_2)] - 1/2E(H_2)$$

where E (AB_2+nH) is the total energy of the AB_2 intermetallic phase with nH atoms per formula unit, E (AB_2) is the energy of the intermetallic AB_2 without H and E (H_2) is half of the energy of an isolated H_2 molecule. With this definition, negative binding energy values correspond to a stable configuration.

The electronic structure and bonding of the hydrides were analyzed by the DOS curves. Bader analysis was used to calculate electronic charges on atoms before and after H absorption [33].

The AB_2 energies, with and without hydrogen, were calculated with the same computational parameters described above. The third term of the E_B expression was determined by locating a H_2 molecule in a cubic cell of 10 Å sides and carrying out a Γ-point calculation, giving a H_2 bond length of 0.751 Å and a binding energy of −4.52 eV, consistent with previous reported values [34,35].

Results and discussion

Table 1 shows all parameters obtained after geometry optimization. Values are in fairly good agreement with other C14 Laves phases [16,36–39]. $Zr_{0.9}Ti_{0.1}(Ni_{0.5}Cr_{0.5})_2$ showed the lowest cell volume and the highest magnetic moment, in relation with Cr atoms amount and their known magnetic properties. The cell volume increases as Cr atoms are substituted by V atoms. Note also that the magnetic moment decreases as the amount of Cr atoms decreases in the cell as expected due the fact that magnetic moment of V atoms is lower than Cr atoms.

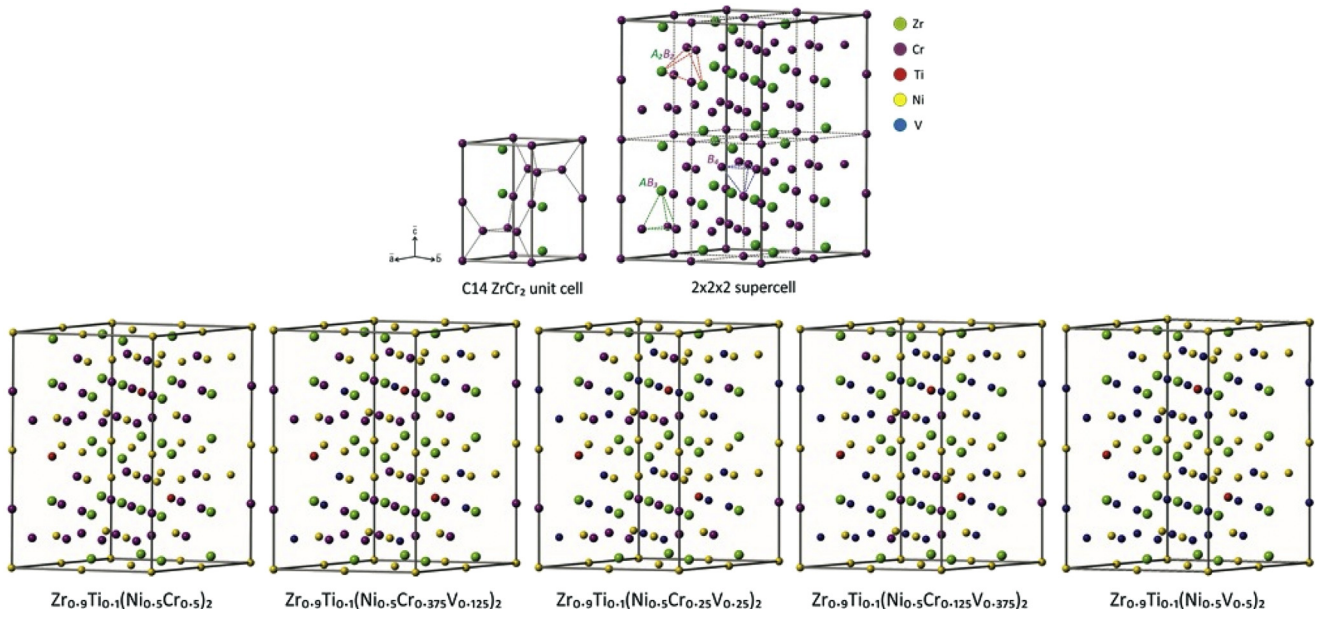

Fig. 1 – C14 Laves phase supercell with all proposed substitutions. Cr atoms content decreases while V atoms content increases.

Table 1 – Lattice parameters, Bulk modulus, cell volume and magnetic moment for the five simulated systems.

	$Zr_{0.9}Ti_{0.1}(Ni_{0.5}Cr_{0.5})_2$	$Zr_{0.9}Ti_{0.1}(Ni_{0.5}Cr_{0.375}V_{0.125})_2$	$Zr_{0.9}Ti_{0.1}(Ni_{0.5}Cr_{0.25}V_{0.25})_2$	$Zr_{0.9}Ti_{0.1}(Ni_{0.5}Cr_{0.125}V_{0.375})_2$	$Zr_{0.9}Ti_{0.1}(Ni_{0.5}V_{0.5})_2$
a = b (Å)	4.990	4.995	5.017	5.039	5.057
c (Å)	8.188	8.197	8.232	8.269	8.298
Bulk modulus (GPa)	149.76	157.73	169.46	150.83	152.24
Cell volume (Å^3)	1412.35	1417.17	1435.60	1454.68	1470.36
Magnetic moment (μ_B)	13.51	10.08	6.70	6.22	1.21

Table 2 – Binding energies (E_B), magnetic moment (μ_B), Cell volume (V) and its difference from the original geometry (ΔV), for all crystals with H atoms absorbed.

		H/F.U.							
		0.75	1.50	2.25	3.00	3.20	3.50	3.75	4.50
$Zr_{0.9}Ti_{0.1}(Ni_{0.5}Cr_{0.5})_2$	Binding energy E_B (eV)	−0.067	−0.083	−0.140	−0.145	−0.141	−0.132	−0.138	−0.141
	Magnetic moment μ (μ_B)	9.437	8.108	4.579	10.847	17.189	9.382	16.421	10.197
	Cell volume V (Å^3)	1461.650	1553.530	1593.380	1644.520	1717.570	1754.630	1765.970	1830.070
	ΔV (%)	4.932	9.996	12.818	16.439	21.611	24.235	25.038	29.576
$Zr_{0.9}Ti_{0.1}(Ni_{0.5}Cr_{0.375}V_{0.125})_2$	E_B	−0.049	−0.112	−0.165	−0.184	−0.166	−0.162	−0.167	−0.166
	μ	7.196	6.007	5.624	7.086	13.096	12.443	14.029	9.199
	V	1524.580	1575.360	1645.610	1702.740	1740.170	1767.460	1782.570	1839.190
	ΔV	7.579	11.162	16.119	20.151	22.792	24.718	25.784	29.779
$Zr_{0.9}Ti_{0.1}(Ni_{0.5}Cr_{0.25}V_{0.25})_2$	E_B	−0.092	−0.144	−0.177	−0.209	−0.193	−0.178	−0.193	−0.193
	μ	7.334	2.819	7.423	6.800	9.824	10.990	12.772	9.695
	V	1516.320	1585.310	1697.170	1736.230	1746.300	1764.830	1804.350	1872.860
	ΔV	5.623	10.428	18.220	20.941	21.643	22.933	25.686	30.458
$Zr_{0.9}Ti_{0.1}(Ni_{0.5}Cr_{0.125}V_{0.375})_2$	E_B	−0.121	−0.174	−0.209	−0.232	−0.214	−0.219	−0.227	−0.224
	μ	5.760	3.577	7.075	6.508	6.886	8.039	9.331	3.053
	V	1530.400	1601.010	1687.250	1735.720	1768.920	1793.840	1804.290	1872.860
	ΔV	5.205	10.059	15.988	19.320	21.602	23.315	24.033	28.747
$Zr_{0.9}Ti_{0.1}(Ni_{0.5}V_{0.5})_2$	E_B	−0.146	−0.199	−0.232	−0.271	−0.237	−0.249	−0.257	−0.115
	μ	2.925	1.450	6.702	3.830	6.373	3.810	7.281	8.424
	V	1548.480	1619.600	1697.170	1731.420	1782.860	1786.320	1808.960	1884.580
	ΔV	5.313	10.150	15.425	17.755	21.253	21.489	23.028	28.171

The value of the strongest E_B for each hydrogenated system is underlined.

Bulk modulus (B) was calculated for each system by fitting the energy-volume data from energy minimization to the Birch-Murnaghan equation of state [40,41], and calculated values are in the range of values informed by different authors [37,38]. All these results indicate a good parametrization of the systems under study.

In order to quantify the H storage capacity for the five systems, the hydrogen binding energy was computed for different numbers of H atoms mostly absorbed in A_2B_2sites -for being the most stable locations in this type of structures and, thus, the first cavities in being occupied by H-but also in AB_3 and B_4 sites, to include and consider some other possible situations.

As in the family of Laves phases it is believed that exist much opportunities for further improvements and they promise hydrogen storage capacities higher than 3.4 H/F.U. [17,21,42], in this opportunity we have proposed to evaluate the energetic behavior of all systems by placing hydrogen atoms into the crystals in an accumulative and random way for different H concentrations beginning from 0.75 H/F.U. up to 4.5 H/F.U. which in our system corresponds to 24 and 144 H atoms respectively.

Table 3 – Average Bader charges for each element after H absorption for the most stable hydrogenated structures. In brackets are indicated the corresponding charge before H absorption. Negative signs indicate an increase in the number of electrons while positive signs, the opposite effect.

	Bader Analysis					
	For hydrogenated systems with the strongest binding energy (3.00 H/F.U)					
	Zr	Ti	Ni	Cr	V	H
$Zr_{0.9}Ti_{0.1}(Ni_{0.5}Cr_{0.5})_2$	+2.383 (2.223)	+1.783 (1.776)	−0.448 (-1.554)	+0.526 (−0.626)	–	−0.802
$Zr_{0.9}Ti_{0.1}(Ni_{0.5}Cr_{0.375}V_{0.125})_2$	+2.352 (2.207)	+1.794 (1.771)	−0.491 (-1.656)	+0.517 (-0.761)	+1.072 (0.244)	−0.821
$Zr_{0.9}Ti_{0.1}(Ni_{0.5}Cr_{0.25}V_{0.25})_2$	+2.353 (2.187)	+1.771 (1.751)	−0.560 (-1.733)	+0.472 (-0.993)	+1.059 (0.167)	−0.835
$Zr_{0.9}Ti_{0.1}(Ni_{0.5}Cr_{0.125}V_{0.375})_2$	+2.334 (2.164)	+1.753 (1.735)	−0.598 (-1.800)	0.407 (-1.121)	+1.013 (-0.058)	−0.847
$Zr_{0.9}Ti_{0.1}(Ni_{0.5}V_{0.5})_2$	+2.341 (2.145)	+1.761 (1.721)	−0.671 (-1.879)	–	+0.998 (-0.226)	−0.871

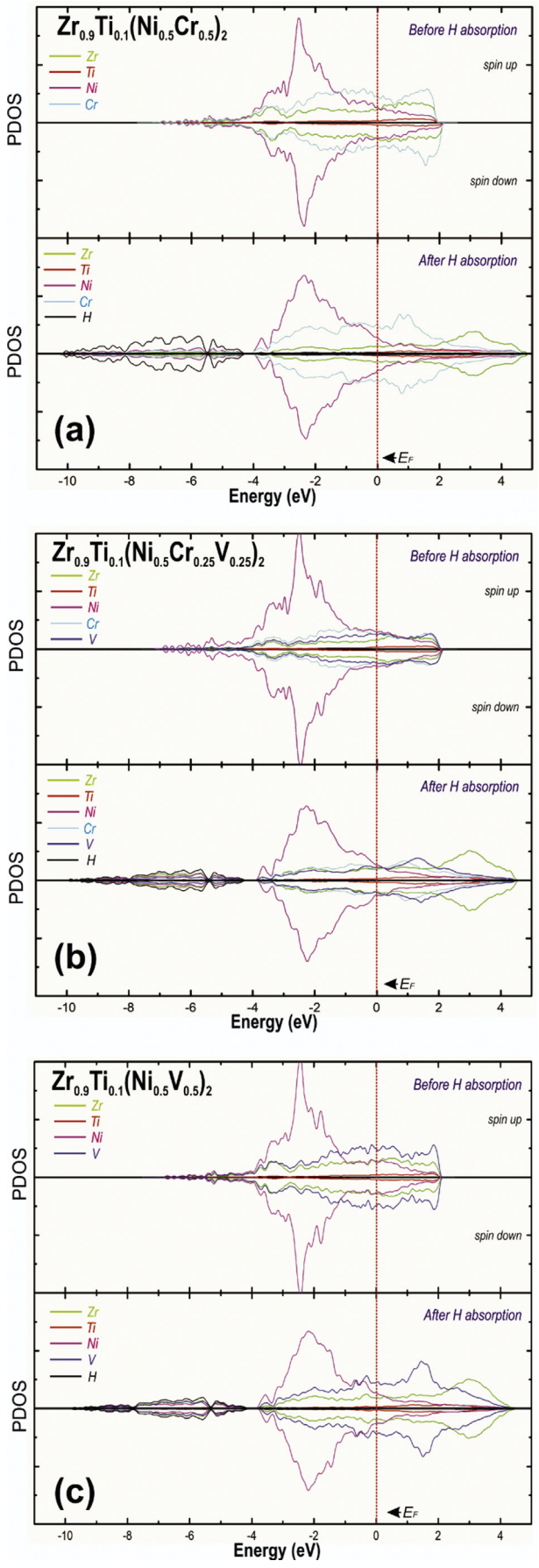

Fig. 2 – PDOS curves for (a) $Zr_{0.9}Ti_{0.1}(Ni_{0.5}Cr_{0.5})_2$, (b) $Zr_{0.9}Ti_{0.1}(Ni_{0.5}Cr_{0.25}V_{0.25})_2$, and (c) $Zr_{0.9}Ti_{0.1}(Ni_{0.5}V_{0.5})_2$ Laves Phases before and after H absorption. Dotted line indicates the Fermi level.

In A_2B_2 sites, H absorbs closer to B type-atoms than to A-type atoms. The distance from H to Zr varies from around 2.05–2.08 Å when both A type atoms in the tetrahedral are Zr atoms. When Ti is part of the tetrahedral sites H is shifted towards Ti and away from Zr (H–Zr ~ 2.25 Å and H–Ti ~ 1.95 Å). Regarding Ni, Cr, and V atoms, H locates at distances around 1.75 Å to 1.85 Å.

Table 2 describes the most relevant data for each system before H absorption. For all structures, H binding energy is smaller for low H concentrations (0.75 and 1.5 H/F.U) and stronger for larger amounts of H absorbed. So according to this calculation results 4.50 H/F.U is still stable but the most favorable configurations is obtained for 3.00 H/F.U corresponding to 96 H atoms absorbed. It can be observed that the binding energy is stronger as more Cr atoms are replaced by V atoms reaching the desired range of metal-to-hydrogen bond strength for higher vanadium contents. Also, as expected, the cell volume increases with H concentration for all structures. The increment is between 5 and 30% and it is observed that it does not depend on the content of vanadium but on the presence of H in the compounds.

3 H/F.U. corresponds to a gravimetric capacity of 1.49 wt% for the $Zr_{0.9}Ti_{0.1}(Ni_{0.5}Cr_{0.5})_2$ and it slightly increases to 1.51 wt% for the alloy where all Cr is replace with vanadium due to V smaller atomic weight. As volume of the cell increases with higher amounts of vanadium the volumetric capacity diminishes from 97.71 to 92.80 g H_2/l. For 4.5 H/F.U. gravimetric capacity can reach 2.27 wt% for the $Zr_{0.9}Ti_{0.1}(Ni_{0.5}V_{0.5})_2$ corresponding to a volumetric capacity of 127.89 g H_2/l. So, although these intermetallic compounds promise an interesting behavior as solid state hydrogen storage materials, their gravimetric capacity does not already reach values reported for the magnesium based hydrides [43,44], which have a high H_2 capacity of 7.6 wt%. However, their main disadvantages lie in the high discharged temperatures (573–673K), slow desorption kinetics and high reactivity toward air and oxygen. Transition-metal-based AB_2-type alloys for metal hydride electrodes, as mentioned before, are often not only multi-element but also multi-component and multi-phase systems. This is due to the flexibility and versatility of the equilibrium plateau pressure produced when varying in a wide range their composition and stoichiometry. Through this *designing concept*, it will possible to compose a material with high gravimetric storage capacity and the suitable thermodynamic conditions to uptake and release hydrogen at ambient conditions.

Electronic structure

Bader charges were calculated for the hydrogenated structures which presented the energetically most favorable configuration; this is the five systems with 3.00 H/F.U. absorbed (underlined in Table 2).

Since H atoms are distributed randomly over the several possible tetrahedral absorption sites available, the average charge for each element was evaluated for all different systems, as shown in Table 3. We analyzed first the atomic charges before H absorption (see values in brackets in Table 3). In all cases Zr and Ti (A type atoms) have a positive charge which remains almost the same for all systems with different amounts of V. Ni on the other hand has a negative charge and is more negative when more V atoms are present. Cr and V also increase their electronic density in systems with a higher amount of V atoms.

When hydrogen is absorbed a redistribution of electronic density is observed. All elements decrease its charge but the change is more noticeably for B type atoms which transfer charge towards hydrogen. Also the charge reduction is increased with the vanadium content in the system. Specifically, Ni loses in average 1.11 e^- in the $Zr_{0.9}Ti_{0.1}(Ni_{0.5}Cr_{0.5})_2$ system and 1.21 e^- in the $Zr_{0.9}Ti_{0.1}(Ni_{0.5}V_{0.5})_2$ where all Cr has been replaced by V. Cr has also a large decrease in the electronic charge: 1.15 e-for the system without V and 1.53 e-in the $Zr_{0.9}Ti_{0.1}(Ni_{0.5}Cr_{0.25}\ V_{0.75})_2$ system. Vanadium also reduces its charge 0.83 e-in $Zr_{0.9}Ti_{0.1}(Ni_{0.5}Cr_{0.75}\ V_{0.25})_2$ and 1.22 e-in $Zr_{0.9}Ti_{0.1}(Ni_{0.5}V_{0.5})_2$.

After electron transfer, H atoms have a negative charge which increases with the V content resulting in a maximum negative charge for hydride with V and no Cr.

Density of states

To complete the study of the electronic structure, the partial density of states (PDOS) projected on each element in the hydride was evaluated for the different systems before H absorption. Finally, a comparison between the density of states before and after H absorption was made for particular cases.

Fig. 2 shows the PDOS on each element composing the system before and after H absorption for three of the systems studied (with no V (a), half Cr atoms substituted with V (b) and all Cr substituted with V (c)). We begin analyzing the systems before H absorption (upper part of Fig. 2 a, b and c). All curves show metallic behavior. In all cases DOS is plotted from −7.2 eV to about 2 eV above the Fermi level. s and p states are spread all over the range of energies while d states concentrate from −4.6 eV up to 2 eV. In particular Ni d states dominates the DOS curves which have a broad band from −4.1 to around −1 eV. Zr and Ti s states start from around −7.2 eV and presents a marked band between −4.5 and −3.0 eV and most of its d states over the Fermi level. The magnetic nature of Cr is shown as the difference between spin up and down states diminishes as Cr is replaced by V. No magnetization is observed for system $Zr_{0.9}Ti_{0.1}(Ni_{0.5}V_{0.5})_2$ where no Cr is present, as expected from magnetic moment calculations above.

The introduction of hydrogen modifies the electronic structure of the host alloy creating metal-hydrogen bonding states (see lower part of Fig. 2 a, b and c). Two bands below the Fermi level starting from around −10 eV appear due to the presence of hydrogen. It can be observed in the figure that the hydride with higher contents of vanadium, increases the contribution of A and B states to the density of states in the lower energy band, increasing the H-M interaction.

Conclusions

Using DFT calculations we have studied hydrogen absorption in $Zr_{0.9}Ti_{0.1}(Ni_{0.5}Cr_{0.5-x}V_x)_2$ Laves Phase, with x = 0, 0.125, 0.25, 0.375, 0.5 in order to determine the influence of V content on H absorption capacity.

The replacement of Cr by V atoms in the system produces a reduction of the magnetic moment of the system and an increase of cell volume resulting in more available space for H absorption.

When H storage is considered it is found that cell volume increases with H concentration. The analysis of binding energy values reveals that for each system the most stable configuration corresponds to a hydrogen concentration of 3.00 H/F.U.

Hydrogen binds stronger with increasing V content in the system. As V content increases E_B reaches the desired range of metal to hydrogen bond strength which ensures the reversibility of the absorbing system.

Bader analysis shows that after H absorption, there is a strong charge transfer from B type atoms towards H. This charge transfer increases with the V content in the system. The higher electron density on H atom could result in a stronger interaction between H and its surroundings.

Regarding density of states, the presence of hydrogen produces a new band at lower energy values between −10 and −4 eV. The increment in V content increases the density of states of A and B elements in this new band, suggesting a reinforcement of H bonding to the system.

Acknowledgements

We acknowledge the financial support given by SGCyT-UNS [PGI 24/F058], and ANPCyT [PICT-2016-4094]. P.Bechthold; A. Juan; C. Pistonesi and M. E. Pronsato are members of CONICET. We kindly acknowledge Federico Lecci, Mechanical Engineering student of the UNPSJB, for his help and time.

REFERENCES

[1] Liu R, Zhang L, Xuellang S, Liu H, Zhang J. Electrochemical technologies for energy storage and conversion. second ed. Germany: Wiley-VCH; 2012.
[2] Sapru K, Reichman B, Reger A, Ovshinsky SR. U.S. Patent 4,623,597. 1986.
[3] Ovshinsky SR, Fetcenko MA, Ross J. A nickel metal hydride battery for electric vehicles. Science 1993;260:176–81.
[4] Ivey DG, Northwood DO. Storing hydrogen in AB_2 Laves-type compounds. Z Phys Chem 1986;147:191–209.
[5] Yongquan L, Xiaoguang Y, Jing W, Qidong W. The electrochemical charge-discharge properties of Zr-Cr-Ni hydrogen storage alloys. J Alloy Comp 2010;231:573–7.
[6] Van Midden HJP, Prodan A, Zupanič E, Žitko R, Makridis SS, Stubos AK. Structural and electronic properties of the hydrogenated $ZrCr_2$ Laves phases. J Phys Chem C 2010;114:4221–7.
[7] Gesari S, Pronsato ME, Visintin A, Juan A. Hydrogen storage in AB_2 Laves phase (A=Zr, Ti; B= Ni, Mn, Cr, V). J Phys Chem 2010;114:16832–6.

[8] Radaković J, Batalović K, Mađarevića I, Belošević-Čavora J. Interstitial hydrogen in Laves phases-local electronic modification from first-principles. Royal Soc Chem 2014;4:54769–74.

[9] Villars P, Calvert LD. Pearson's handbook of crystallographic data for intermetallic phases. second ed. Ohio: American Society for Metals; 1991.

[10] Pearson WB. The crystal chemistry and physics of metals and alloys. first ed. New York: John Wiley & Sons Inc; 1972.

[11] Westbrook JH. Intermetallic compounds. first ed. New York: R. E. Krieger Pub. Co; 1977.

[12] Kasper JS. Theory of alloy phases. first ed. Ohio: American Society for Metals; 1956.

[13] Christen HR. Fundamentos de la química general e inorgánica. first ed. Barcelona: Reverté; 1986.

[14] Johnston RL, Hoffman R. Structure-bonding relationships in the Laves phases. Z Anorg Allg Chem 1992;616:105–20.

[15] Shoemaker DP, Shoemaker CB. Concerning atomic sites and capacities for hydrogen absorption in the AB_2Friauf-Laves phases. J Less Common Met 1979;68:43–58.

[16] Robina Merlino A, Luna CR, Juan A, Pronsato ME. A DFT study of hydrogen storage in $Zr(Cr_{0.5}Ni_{0.5})_2$ Laves Phase. Int J Hydrogen Energy 2015;41:2700–10.

[17] Yang XG, Lei YQ, Zhang WK, Zhu GM, Wang QD. Effect of alloying with Ti, V, Mn on the electrochemical properties of Zr-Cr-Ni based Laves phase metal hydride electrodes. J Alloy Comp 1996;243:151–5.

[18] Verbetsky VN, Petrii OA, Vasina SY, Bespalov AP. Electrode materials based on hydrogen-sorbing alloys of AB_2 composition (A=Ti,Zr; B=V, Ni, Cr). Int J Hydrogen Energy 1999;24:247–9.

[19] Visintin A, Peretti HA. Hydrogen absorption characteristics and electrochemical properties of Ti substituted Zr-based AB_2 alloys. Int J Hydrogen Energy 2001;26:683–9.

[20] Peretti HA, Visintin A, Mogni LV, Corso HL, Andrade Gamboa J, Serafini D, et al. Hydrogen absorption behaviour of multicomponent zirconium based AB_2 alloys with different chromium-vanadium ratio. J Alloy Comp 2003;354:181–6.

[21] Bououdina M, Enoki H. The investigation of the $Zr_{1-y}Ti_y(Cr_{1-x}Ni_x)_2$-$H_2$ system $0\leq y\leq 1$ and $0\leq x\leq 1$. Phase composition analysis and thermodynamic properties. J Alloy Comp 1998;281:290–300.

[22] Soubeyroux JL, Bououdina M, Fruchart D, Pontonnier L. Phase stability and neutron diffraction studies of Laves phases $Zr(Cr_{1-x}M_x)_2$ with M=Mn, Fe, Co, Ni, Cu and $0<x<0.2$ and their hydrides. J Alloy Comp 1995;219:48–54.

[23] Züttel A, Chartouni D, Gross K, Bächler M, Schlapbach L. Structural and hydriding properties of the $Zr(V_{0.25}Ni_{0.75})_\alpha$ ($1\leq \alpha \leq 4$) alloy system. J Alloy Comp 1997;587:253–4.

[24] Agostino RG, Liberti G, Formoso V, Colavita E, Züttel A, Nützenadel C, et al. In situ x-ray absorption study of $Zr(V_{0.29}Ni_{0.71})_3$ hydride electrodes. Phys Rev B 2000;61:13647–54.

[25] Bououdina M, Menier P, Soubeyroux JL, Fruchart D. Study of the system $Zr_{1-x}Ti_x(Cr_{0.5}M_{0.4}V_{0.1})_2 - H_2$ ($0\leq x \leq 0.2$, M=Fe, Co, Ni). J Alloy Comp 1997;253:302–7.

[26] Kim DM, Jeon SW, Lee JY. A study of the development of a high capacity and high performance Zr–Ti–Mn–V–Ni hydrogen storage alloy for Ni–MH rechargeable batteries. J Alloy Comp 1998;279:209–14.

[27] G. Kresse, J. Furthmüller. http://cms.mpi.univie.ac.at/vasp/vasp/vasp.html.

[28] Kresse G, Hafner J. Ab initio molecular dynamics for liquid metals. Phys Rev B 1993;47:558–61.

[29] Kresse G, Furthmüller J. Efficient iterative schemes for ab initio total-energy calculations using a plane-wave basis set. Phys Rev B 1996;54:11169–86.

[30] Kresse G, Furthmüller J. Efficiency of ab-initio total energy calculations for metals and semiconductors using a plane-wave basis set. Comp Mater Sci 1996;6:15–50.

[31] Kresse G, Joubert D. From ultrasoft pseudopotentials to the projector augmented-wave method. Phys Rev B 1999;59:1758–75.

[32] Perdew J, Burke K, Ernzerhof M. Generalized gradient approximation made simple. Phys Rev Lett 1996;77:3865–8.

[33] Bader R. Atoms in molecules. A quantum theory. first ed. Oxford: Clarendon Press; 1990.

[34] Vajeeston P, Ravindran P, Vidya R, Kjekshus A, Fjellvag H. Site preference of hydrogen in metal, alloy and intermetallic frameworks. Europhys Lett 2005;72:569–75.

[35] Al Alam AF, Matar SF, Ouaïni N, Nakhl M. Hydrogen insertion effects on the magnetic properties and chemical bonding within C14 Laves phases. Prog Solid State Chem 2008;36:192–212.

[36] Bououdina M, Soubeyroux JL, Fruchart D, de Rango P. Structural studies of Laves phases $Zr(Cr_{1-x}Ni_x)_2$ with $0\leq x\leq 0.4$ and their hydrides. J Alloy Comp 1997;257:82–90.

[37] Xing-Qiu Chen, Wolf W, Podloucky R, Rogl P. Ab initio study of ground-state properties of the Laves phase compounds $TiCr_2$,$ZrCr_2$, and $HfCr_2$. Phys Rev B 2005;71:174101–11.

[38] Sun J, Jiang B. Ab initio calculation of the phase stability, mechanical properties and electronic structure of $ZrCr_2$ Laves phase compounds. Philos Mag A 2004;84:3133–44.

[39] Nagasako N, Fukumoto A, Miwa K. First-principles calculations of C14-type Laves phase Ti-Mn hydrides. Phys Rev B 2002;66:155106–9.

[40] Birch F. The effect of pressure upon the elastic parameters of isotropic solids, according to murnaghan's theory of finite strain. J Appl Phys 1938;9:279288.

[41] Birch F. Finite elastic strain of cubic crystals. Phys Rev 1947;71:809–24.

[42] Soubeyroux JL, Fruchart D, Biris AS. Structural studies of Laves phases $ZrCo(V_{1-x}Cr_x)$ with $0<x<1$ and their hydrides. J Alloy Comp 1999;293:88–92.

[43] Bhihi M, El Khatabi M, Lakhal M, Naji S, Labrim H, Benyoussef A, et al. First principle study of hydrogen storage in doubly substituted Mg based hydrides. Int J Hydrogen Energy 2015;40:8356–61.

[44] Abdellaoui M, Lakhal M, Bhihi M, el Khatabi M, Benyoussef A, El Kenz A, et al. First principle study of hydrogen storage in doubly substituted Mg based hydrides Mg_5MH_{12} (M=B, Li) and Mg_4BLiH_{12}. Int J Hydrogen Energy 2016;41:20908–13.